Journal of Software Engineering, 2015
ISSN 1819-4311 / DOI: 10.3923/jse.2015.

Research on the Steady State and Ripple Current Models of Current Mode Switching Power Amplifier for Magnetic Bearing

[1]Jun Wang, [2]Liping Wang, [2]Jianghui Dong and [1]Cong Huang
[1]College of Information Science and Technology, Nanjing Forestry University, Nanjing 210037, China
[2]School of Computer Science, Engineering and Mathematics, Flinders University, South Australia 5042, Australia

Corresponding Author: Jun Wang, College of Information Science and Technology, Nanjing Forestry University, Nanjing 210037, China

ABSTRACT

The current mode switching power amplifier is an essential component in magnetic bearing system which works in the nonlinear switching state. At present, the characteristics of the power amplifier can be revealed partially by establishing first order inertial element model. In order to accurately investigate the actual working characteristics of the current mode power amplifier, a precise mathematical model of switching power amplifier is proposed based on the circuit principle and Fourier series analysis method. In the analysis of the current forming principle for three-level Pulse Width Modulation (PWM) power amplifier, the load coil voltage is deduced by Fourier series method. The steady state current model and ripple current model are established, respectively. Compared with the model simulation and experiment, the results show that the characteristics of the ripple current, steady state and dynamic state are basically consistent. We found that the model predictions results are in excellent agreement with the actual experiments data, indicating the numerical simulations model is feasible and effective for the design of power amplifier system.

Key words: Switching power amplifier, magnetic bearing, steady state, ripple current, current mode

INTRODUCTION

Magnetic bearing is a bearing system supported by magnetic levitation without the physical contact of the rotor. It has many advantageous features compared with the conventional mechanical bearing system, such as low friction, high efficiency and no mechanical wear (Looser and Kolar, 2014; Saeed *et al*., 2013; Zhong and Zhu, 2013; Chen and Lin, 2013; Radhakrishna *et al*., 2013; Ji *et al*., 2013). Magnetic bearing system has been widely used in different areas of high speed motor, compressor, flywheel energy storage (Ji and Xu, 2012; Barbaraci *et al*., 2013; Park, 2014; Fang *et al*., 2010; Sun and Fang, 2011; Tiwari and Chougale, 2014) and current mode power amplifier is one of most important parts of electrically controlled system in magnetic bearing. The power amplifier provides sufficient current for radial and axial bearing coil to produce the desired electromagnetic forces (Fang and Ren, 2012; Zhou *et al*., 2012). In order to stabilize the dynamic vibrations of high speed bearing system, the power amplifier has to meet the specific requirements, such as high frequency bandwidth, small current distortion and magnetic bearing.

The three-level switching power amplifiers are widely used for high precision control of magnetic bearings system due to its low power loss and small current ripple compared with the linear power amplifier or two-level switching power amplifier (Zhou and Zhu, 2010a, b; Ren and Fang, 2012; Fan *et al.*, 2013; Chang *et al.*, 2010).

Three-level power amplifier circuit is a nonlinear system as the devices including power Metal-Oxide-Semiconductor Field-Effect Transistors (MOSFETs) and diodes operate in switching state (Wang and Xu, 2010a). So, power amplifier cannot be analyzed by conventional methods (such as the Laplace transform method) to resolve the circuit as linear constant systems. For better understanding the working principle and circuit results, previous researches of the simulation models for switching power amplifier in magnetic bearing system focused on professional circuit software simulation. Yu *et al.* (2010) used Power System Blockset (PSB) model library of MATLAB or Pspice software for the modeling and simulations, in which the specific components of the circuit model can be selected while the simulation interface is simple and concise (Zhang *et al.*, 2005). Although the method doesn't require to be derived from a mathematical model, no clear physical concept can be presented in this method. Based on a state-space averaging method, Wang and Xu (2009a) established a math model of power amplifier and analyzed the closed-loop system transfer function. A uniform equivalent circuit mode of power amplifier is obtained after the small signal perturbations and linear processing (Wang and Xu, 2009a). Wang and Xu (2009b) used the equivalent switching model method and the switching half bridge circuits were presented as three-terminal nonlinear devices. It can be linearized by averaging circuit method under the principle of energy conversion (Wang and Xu, 2009b). These methods cannot investigate the output current ripple size effectively as the switching frequency factor was ignored. Based on the three-level PWM operating principle of output load current, Wang and Xu (2010b) proposed the mathematical model of switching power amplifier based on Fourier analysis methods. This method can analyze the characteristics of Alternating Current (AC) and Direct Current (DC) power amplifier system which is derived from ideal conditions of circuit parameters without considering the effects of switch device and other diode voltage. As these methods cannot characterize the actual properties of the power amplifier, it is necessary to establish an accurate model derived from actual parameters of devices.

In this study, a new universal mathematical modeling method is derived from the analysis of three-level Pulse Width Modulation (PWM) switching power amplifier circuit theory and the output voltage expressed as a Fourier series method. According to this model, the system structure diagram is deduced by actual component parameters. The steady state transfer function and current ripple mathematical function are obtained. Finally, the simulations and experiments are also carried out to verify the effectiveness of the proposed model in both in steady state and dynamic state.

PRINCIPLES OF THREE-LEVEL PWM SWITCHING POWER AMPLIFIER

The schematic of switching power amplifier system is shown in Fig. 1. The system consists of four switching devices with S_1, S_2, S_3 and S_4, four diodes with D_1, D_2, D_3 and D_4, load inductor L and other three auxiliary control circuits. Notice that the analysis principle of unidirectional current power amplifier is similar to bidirectional current amplifier circuit. As an example, a common mathematical model of unidirectional current three-level power amplifier is presented in this study.

Circuit analysis: For a three-level power amplifier circuit, analysis is performed for four distinct operating modes as shown in Fig. 2. Different mode processes are given as follows:

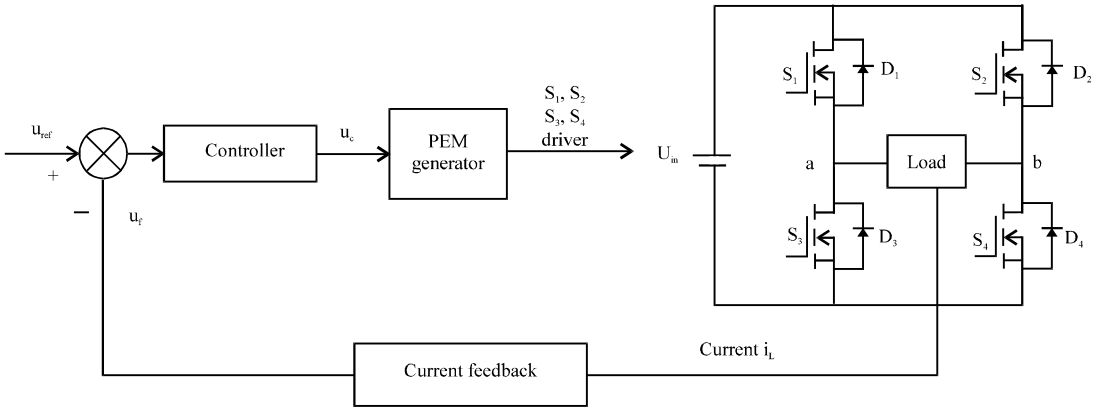

Fig. 1: Schematic of switching power amplifier system

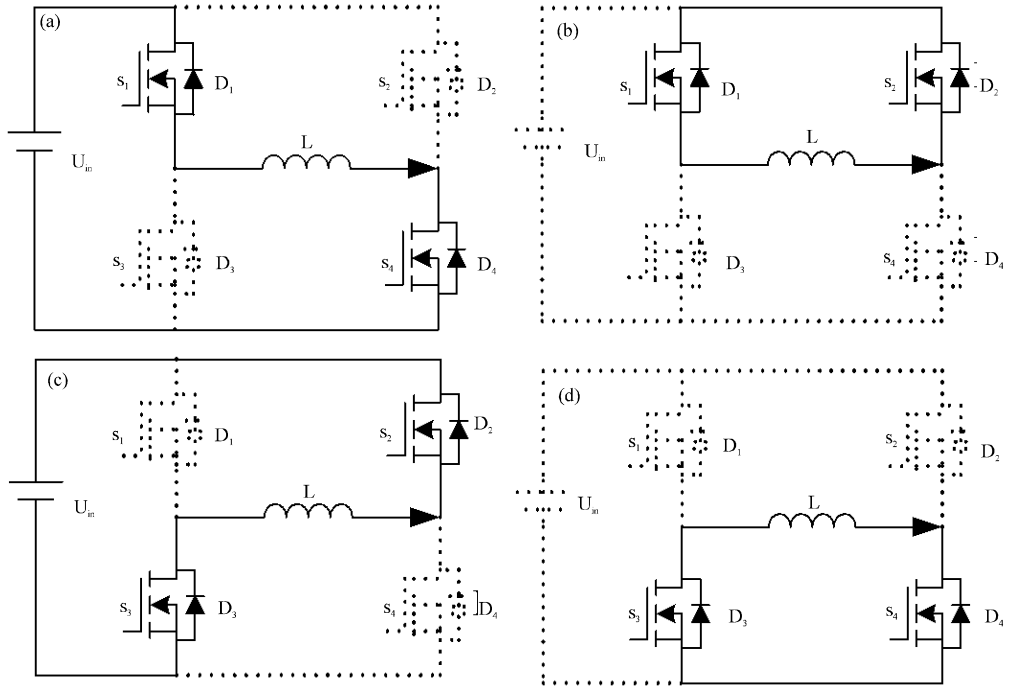

Fig. 2(a-d): Mode diagrams of three-level power amplifier operation in which inductor current, (a) Increase, (b) Continous to flow, (c) Decreases linearly and (d) Still continous to flow

At mode 1, the inductor current increases linearly as shown in Fig. 2(a). The output load current i_L flows through switch S_1 and S_4. The switch S_2 and S_3 are in off state. The function of the inductor and DC source U_{in} is determined as below:

$$U_L + ri_L + 2U_{on} = U_{in} \tag{1}$$

where, U_L is the inductor voltage, r is the resistor of inductor coil, U_{on} is the conducting voltage across the switching devices.

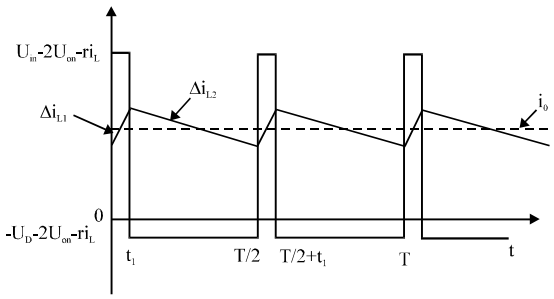

Fig. 3: Output current waveform in steady state work

At mode 2, the inductor current continues to flow as shown in Fig. 2(b). The switch S_1 and diode D_2 are in on state. The switch S_3 and S_4 are in off state. U_D is the diode forward voltage. The equation of this mode is expressed as:

$$U_L + ri_L + U_{on} + U_D = 0 \tag{2}$$

At mode 3, the inductor current decreases linearly as shown in Fig. 2(c). The output current flows through switch S_2 and S_3. The switch S_1 and S_4 are in off state. The function can be expressed as below:

$$U_L + ri_L + 2U_{on} = -U_{in} \tag{3}$$

At mode 4, the inductor current still continues to flow as shown in Fig. 2(d). The switch S_1 and S_2 are in off state. The diode D_3 and switch S_4 are in on state. The equation is expressed as:

$$U_L + ri_L + U_{on} + U_D = 0 \tag{4}$$

The output current waveform in steady state work is shown in Fig. 3. When the three-level switching power amplifier works steady in a cycle time, there are only two operating states. In mode 1, load current increases slightly to compensate for the current flow loss. In mode 2 or mode 4, load current reduces slightly under the conducting voltage across the switching devices and diode forward voltage.

Analysis of output current ripple: According to the inductor voltage-second balance principle, the change of increasing inductor current Δi_{L1} is equal to the change of decreasing inductor current Δi_{L2} as shown in Fig. 3. In the period from 0 to t_1, the equation can be calculated as:

$$\Delta i_{L1} = \int_0^{t_1} \frac{U_{in} - 2U_{on} - ri_L}{L} dt = \frac{U_{in} - 2U_{on} - ri_L}{L} t_1 \tag{5}$$

In the period from t_1 to T/2, the inductor current is in mode 2 or mode 4, so the current change equation can be obtained as:

$$\Delta i_{L2} = -\int_{t_1}^{T/2} \frac{U_{on} + U_D + ri_L}{L} dt = -\frac{U_{on} + U_D + ri_L}{L}\left(\frac{T}{2} - t_1\right) \tag{6}$$

As the current changes are both to equal, the switching conduction time t_1 is shown as follows:

$$t_1 = \frac{U_{on} + U_D + ri_L}{(U_{in} - U_{on} + U_D)} \cdot \frac{T}{2} \tag{7}$$

It is well known that the time of DC voltage across the inductor is constant when these parameters of DC voltage, switching devices conducting voltage, diode forward voltage and coil resistor are determined (Wang and Xu, 2010b). This conclusion provides the analysis foundation of modeling three-level PWM switching amplifier.

NONLINEAR MODEL OF THREE-LEVEL SWITCHING POWER AMPLIFIER

Individual sub-system model: Based on the Kirchhoff's voltage law, the relationship between the load voltage u_{ab} and load current i_L is derived as:

$$u_{ab} = i_L(r + Ls) \tag{8}$$

The loop of current feedback converts the load current signal to a voltage signal, usually using a current sampling resistor or a hall current sensor. It works in linear mode and current feedback gain is constant h. Therefore, this part model function is expressed as:

$$u_f = hi_L \tag{9}$$

Controller can rapidly regulate the output control signal in response to the error voltage. At the same time, it provides adequate gain margin and phase margin for power amplifier. The controller is usually achieved by the operational amplifier circuit and the model is expressed as follows:

$$u_c = \frac{R_1Cs + 1}{R_2Cs} u_e \tag{10}$$

where, R_1 and R_2 are the resistors, C is the compensation capacitor.

For a full bridge circuit, conducting voltages across the switching devices and diode forward voltages are considered, the relationship of voltage u_{ab} can be expressed as:

$$u_{ab} = \begin{cases} U_{in} - 2U_{on} & nT/2 \le t \le nT/2 + t_1 \\ -U_{on} - U_D & nT/2 + t_1 \le t \le (n+1)T/2 \end{cases} \tag{11}$$

The voltage u_{ab} expressed as Fourier series is defined as:

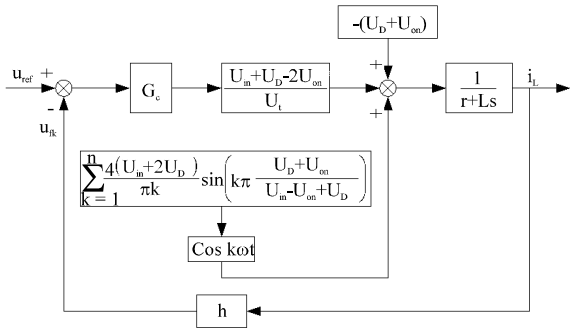

Fig. 4: Block diagram of nonlinear system model for three-level switching power amplifier

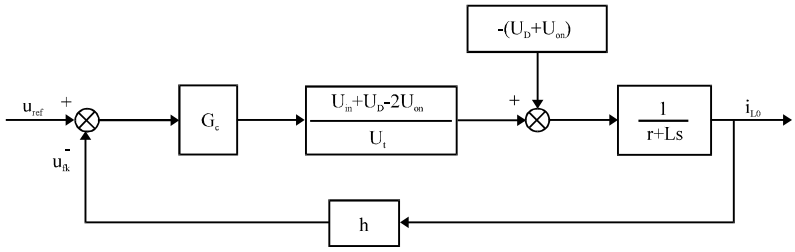

Fig. 5: Steady-state current model of three-level switching power amplifier

$$u_{ab}=\frac{U_{in}+U_D-U_{on}}{U_t}u_c-(U_D+U_{on})+\sum_{k=1}^{\infty}\frac{4(U_{in}+2U_D)}{k\pi}\sin\left(k\pi\frac{U_D+U_{on}}{U_{in}+U_D-U_{on}}\right)\cos(k\omega t) \tag{12}$$

The first term in Eq. 12 is a DC constant term and determines steady state value of the load current. U_c is the controller output voltage signal and U_t is the amplitude of the PWM triangular carrier. The second term is the cosine accumulate term that decides the size of load current ripple.

Block diagram of nonlinear system model for three-level PWM switching power amplifier with the above sub-system models were shown in Fig. 4.

From Fig. 4, there are three input signals affecting to the output current in the system. The given reference voltage u_{ref} is proportional to the steady state current of load coil. The second input $-(U_D+U_{on})$ is the interference term for steady-state current. The last input is the cosine accumulate term which affects the output current ripple in the three-level PWM power amplifier. System model is divided into steady-state current model and ripple current model. Output current equation of power amplifier is derived by superposition principle:

$$i_L(t)=L^{-1}(i_{L0}(s)+i_{Lw}(s))*u_{ref}(t) \tag{13}$$

Analysis of the steady-state current model: Considering the two inputs of u_{ref} and $-(U_D+U_{on})$, the steady-state current model of three-level switching power amplifier is shown in Fig. 5.

Both of the transfer functions of two inputs are deduced by:

$$G_1(s)=\frac{i_{L01}(s)}{u_{ref}(s)}=\frac{1}{h}\cdot\frac{R_1Cs+1}{\frac{LR_2CU_t}{h(U_{in}+U_D-U_{on})}s^2+\left(\frac{rR_2CU_t}{h(U_{in}+U_D-U_{on})}+R_1C\right)s+1} \tag{14}$$

$$G_2(s)=\frac{i_{L02}(s)}{u(s)}=\frac{1}{(U_{in}+U_D-U_{on})h}\cdot\frac{U_tR_2Cs}{\frac{LR_2CU_t}{h(U_{in}+U_D-U_{on})}s^2+\left(\frac{rR_2CU_t}{h(U_{in}+U_D-U_{on})}+R_1C\right)s+1} \tag{15}$$

The steady-state current equation can be deduced from Eq. 14 and 15 as:

$$\begin{aligned}i_{L0}(s)=i_{L01}(s)+i_{L02}(s)=&\frac{1}{h}\cdot\frac{R_1Cs+1}{\frac{LR_2CU_t}{h(U_{in}+U_D-U_{on})}s^2+\left(\frac{rR_2CU_t}{h(U_{in}+U_D-U_{on})}+R_1C\right)s+1}\cdot u_{ref}(s)\\&+\frac{1}{(U_{in}+U_D-U_{on})h}\cdot\frac{U_tR_2Cs}{\frac{LR_2CU_t}{h(U_{in}+U_D-U_{on})}s^2+\left(\frac{rR_2CU_t}{h(U_{in}+U_D-U_{on})}+R_1C\right)s+1}\cdot(-U_D-U_{on})\end{aligned} \tag{16}$$

Analysis of the ripple current model: Considering the cosine accumulate voltage, the ripple current model of three-level switching power amplifier is shown in Fig. 6.

The transfer function of ripple current model is deduced as:

$$\begin{aligned}i_{Lw}(s)=&\frac{1}{(U_{in}+U_D-U_{on})h}\cdot\frac{U_tR_2Cs}{\frac{LR_2CU_t}{h(U_{in}+U_D-U_{on})}s^2+\left(\frac{rR_2CU_t}{h(U_{in}+U_D-U_{on})}+R_1C\right)s+1}\cdot\\&\left(\sum_{k=1}^{\infty}\frac{4(U_{in}+2U_D)}{k\pi}\sin\left(k\pi\frac{U_D+U_{on}}{U_{in}+U_D-U_{on}}\right)\cos(k\omega t)\right)\end{aligned} \tag{17}$$

MATERIALS AND METHODS

Simulation: In this section, simulations are carried out for the proposed power amplifier model using simulink program as the verification of the previous analysis. The conducting voltages of switching devices S_1, S_2, S_3, S_4 are 0.7 V and diode forward voltage is 0.8 V. The amplitude voltage of triangular carrier is 13 V. Other parameters of the circuit are U_{in} = 50 V, R_1 = 20 kΩ, R_2 = 10 kΩ, C = 0.1 μF, r = 2 Ω, L = 1.2 mH and h = 5.

Experiment: In this section, experiments are carried out to verify the previous simulation model analysis.

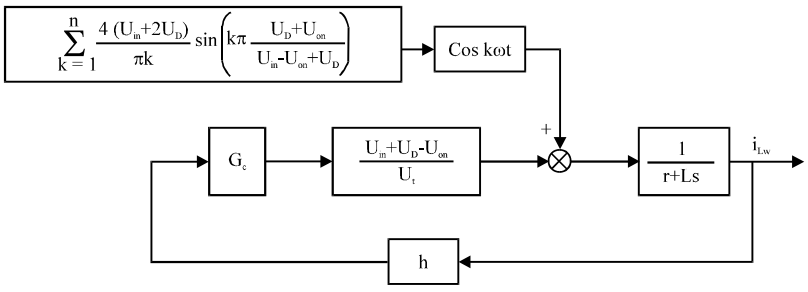

Fig. 6: Ripple current model of three-level switching power amplifier

The four switching devices are module type IRFP460 MOSFETs and the four diodes are MUR860. Two single MOSFETs are series for each phase-leg and each MOSFET is anti-paralleled with an ultra-fast diode. The following figures are drawn according to the data captured by Tektronix digital oscilloscope. Hall current sensors are used in the experiments to detect the coil current with the sensitivity of 5 V mA^{-1}.

RESULTS AND DISCUSSION

Simulation waveforms of output current model for three-level PWM switching power amplifier are shown in Fig. 7. Figure 7a is simulation waveform of ripple current. The current ripple is expressed by Eq. 17 which is based on the first four major components of harmonic. This is due to five times or more harmonic components with higher frequencies occupy a small proportion of the ripple current. Peak to peak value of ripple current is about 72 mA, whilst the theoretical value of calculation is 70 mA. The error between the calculated and theoretical value is 2.86%. Figure 7b is simulation output current waveform under the conditions of the input 5 V voltage and output 1 A current. The average current observed from figure is stabilized at 1 A. There is no error

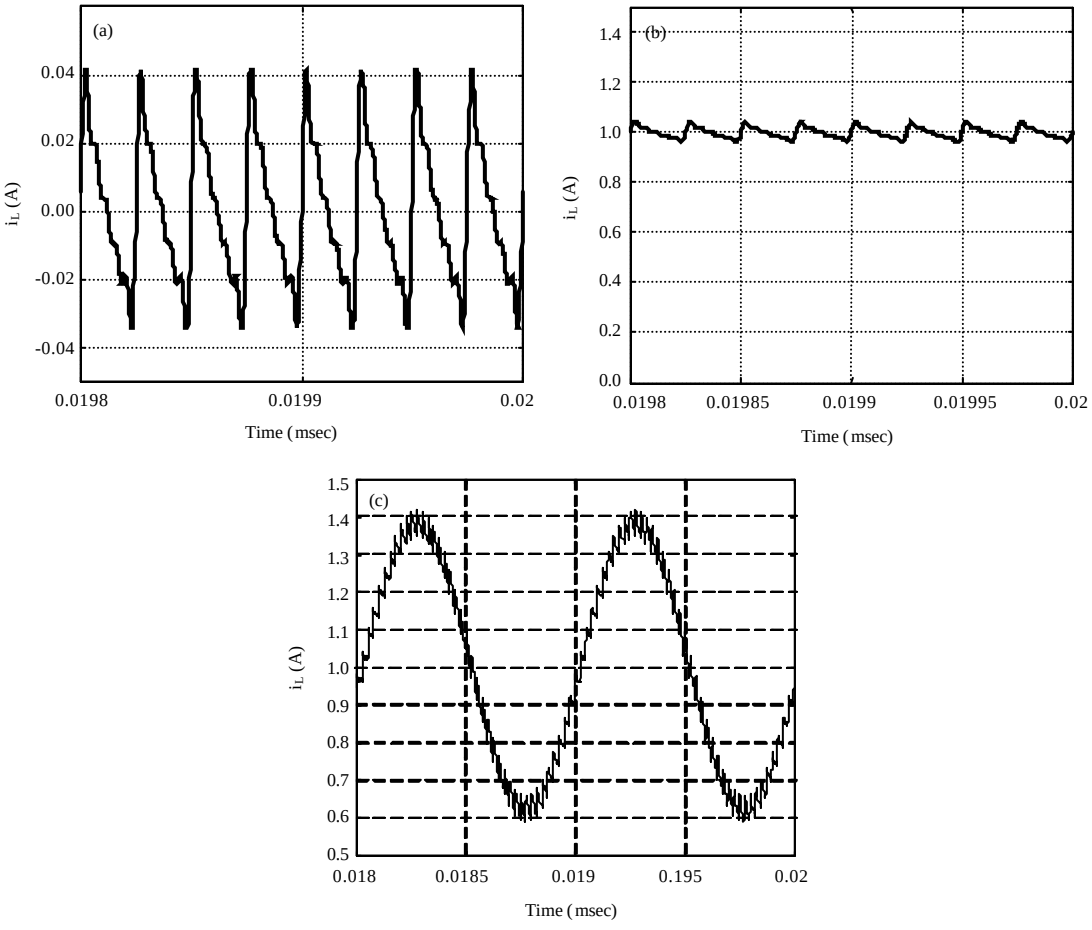

Fig. 7(a-c): Simulation waveforms of output current model for three-level PWM power amplifier, (a) Simulation waveform of ripple current, (b) Simulation current waveform under input 5V voltage and (c) Simulation current waveform of dynamic characteristic

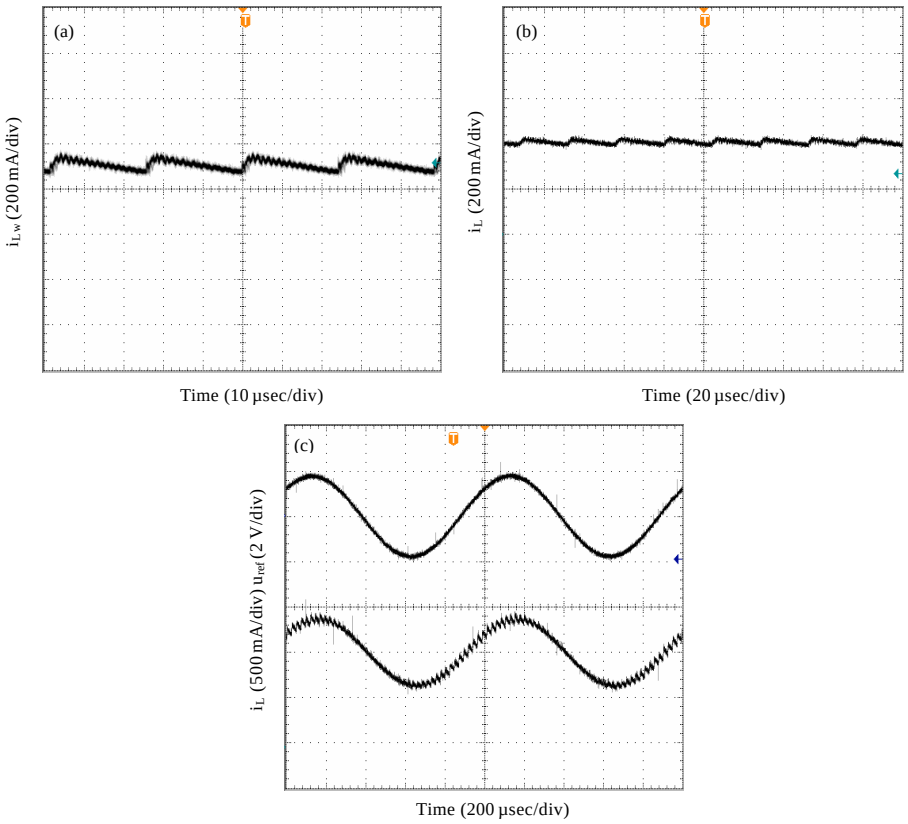

Fig. 8(a-c): Experimental current waveforms of three-level power amplifier, (a) Experiment waveform of ripple current, (b) Experiment current waveform under input 5 V voltage and (c) Experiment current waveform of dynamic characteristic

observed in average current. Figure 7c is to validate the model of dynamic characteristic waveforms at high speed. The input peak value of sinusoidal voltage signal is 4 V and sinusoidal frequency is 1000 Hz to power amplifier. The theoretical calculation peak value of dynamic current is 0.8 A and the simulation peak value of the dynamic current is 0.81 V which is a 1.25% error between them.

From these simulation waveforms, the load coil current is superimposed on the steady state current and ripple current. The average values of the steady state current are not affected by the ripple current. Ripple current is only associated with the circuit parameters of switch conducting voltage, diode forward voltage, load inductor and resistor. The ripple current is not related to the DC voltage directly but with the decline of the switching frequency, the ripple currents increase proportionally. Simulation results are in good agreement with that obtained from theoretical analysis.

Figure 8a is an experiment waveform of ripple current. The actual peak to peak value of ripple current from experiment is about 70 mA which is consistent with the theoretical value. The experiment result has an error of 2.86% compared with the simulation result. Figure 8b is experimental output current waveform under the conditions of the input 5 V voltage and output 1 A current. The actual value of stable current is 1 A, consistent with the simulation model results.

Figure 8c is experiment dynamic characteristic waveforms at high speed. The input peak value of sinusoidal voltage signal is still 4 V and sinusoidal frequency is 1000 Hz. The actual measured change value of peak current is 0.8 A. The theoretical calculation peak value of dynamic current is 0.8 A. The error of simulation result is 1.25% compared with the experimental results.

Compared with the waveforms simulated by the proposed model, the ripple results of experimental testing are basically the same. Three-level switching power PWM amplifier has a much smaller current ripples than two-level switching power amplifier that value of current ripples is 0.8 A. For dynamic response, evaluation standards are the amplitude size and phase delay, the output current signals have the same amplitude and can quickly track the input sinusoidal signals. The phase lag of output current is about 8°. Experiment is validating the method to establish the nonlinear system model of switching power amplifier. New model proposed for switching power amplifier is accurately analyzed steady-state current and ripple current which can demonstrate the dynamic characteristics of the actual power amplifier effectively.

As this study attempts to investigate the actual working characteristics in the field of the current mode power amplifier, there are several implications that could be drawn from the obtained findings. First, compared to Yu *et al.* (2010) and Zhang *et al.* (2005) previous studies, this present study establishes a precise high order mathematical model for the first time. The new model of output current includes steady-state current and ripple current. Therefore, the presented model has a superior target to get global characteristics of power amplifier. This new study presents a clear physical concept which previously published studies have not proposed. So, the result is in agreement with actual state.

Second, there is impossibility to have ripple current model in some previously published studies (Wang and Xu, 2009a, b, 2010b). This present study first considers the factors of switching frequency which other above articles are incorrectly ignored. Based on circuit principles and Fourier series method, the effects of device forward voltages are first analyzed for predicting the characteristics of the power amplifier. The result of experiment has an error of 2.86% compared with previous studies.

CONCLUSIONS

In this study, the circuit theory and Fourier series are used to analyze the state and the harmonic model for nonlinear closed loop system in three-level PWM switching power amplifier. The steady-state current model and ripple current model of the closed loop system were established. The transfer function of different models was derived and simulation model was verified by experiments results. Model of nonlinear switching power amplifier can accurately demonstrate the steady state output current and dynamic characteristics for power amplifier system. It can not only guide the optimal design parameters of the power amplifier but also provide a theoretical analysis tool for the magnetic levitation control system.

ACKNOWLEDGMENTS

This study is supported by National Nature Science Foundation of China (Grant No. 51275240), the Natural Science Foundation of the Jiangsu Higher Education Institutions of China (Grant No. 13KJB510014), the Enterprise Doctor Gathering Plan of Jiangsu Province (Grant No. 2012165) and the practice innovation training program project of the Jiangsu College students (Grant No. 201410298028Z).

REFERENCES

Barbaraci, G., G.V. Mariotti and A. Piscopo, 2013. Active magnetic bearing design study. J. Vibr. Control, 19: 2491-2505.

Chang, X., L. Xu and J. Dong, 2010. [Digital power amplifier of active magnetic bearing]. J. Mech. Eng., 46: 9-14, (In Chinese).

Chen, S.Y. and F.J. Lin, 2013. Decentralized PID neural network control for five degree-of-freedom active magneticbearing. Eng. Applic. Artif. Intell., 26: 962-973.

Fan, Y.P., S.Q. Liu, H.W. Li, Y.P. Zhang and Y.J. Dai, 2013. Time delay compensation of switching power amplifier for magnetic bearing based on DOB. Electr. Mach. Control, 17: 103-107.

Fang, J. and Y. Ren, 2012. Self-adaptive phase-lead compensation based on unsymmetrical current sampling resistance network for magnetic bearing switching power amplifiers. IEEE Trans. Ind. Electron., 59: 1218-1227.

Fang, J., J. Sun, H. Liu and J. Tang, 2010. A novel 3-DOF axial hybrid magnetic bearing. IEEE Trans. Magn., 46: 4034-4045.

Ji, L. and L. Xu, 2012. Research on an inverter-fed six-pole permanent magnet biased magnetic bearing. Proceedings of the 13th International Symposium on Magnetic Bearings, August 9-11, 2012, Arlington, USA.

Ji, L., L. Xu and C. Jin, 2013. Research on a low power consumption six-pole heteropolar hybrid magnetic bearing. IEEE Trans. Magne., 49: 4918-4926.

Looser, A. and J. Kolar, 2014. An active magnetic damper concept for stabilization of gas bearings in high-speed permanent-magnet machines. IEEE Trans. Ind. Electron., 61: 3089-3098.

Park, Y., 2014. Design and implementation of an electromagnetic levitation system for active magnetic bearing wheels. IET Control Theory Applic., 8: 139-148.

Radhakrishna, M., S. Jana, B.K. Sreedhar, P. Kalyanasundaram and V.A. Kumar, 2013. Development of active magnetic bearings for a vertical centrifugal pump rotor. Adv. Vibr. Eng., 12: 329-335.

Ren, Y. and J. Fang, 2012. Current-sensing resistor design to include current derivative in PWM H-bridge unipolar switching power amplifiers for magnetic bearings. IEEE Trans. Ind. Electron., 59: 4590-4600.

Saeed, N.A., M. Eissa and W.A. El-Ganini, 2013. Nonlinear oscillations of rotor active magnetic bearings system. Nonlinear Dyn., 74: 1-20.

Sun, J. and J. Fang, 2011. A novel structure of permanent-magnet-biased radial hybrid magnetic bearing. J. Magnetism Magn. Mater., 323: 202-208.

Tiwari, R. and A. Chougale, 2014. Identification of bearing dynamic parameters and unbalance states in a flexible rotor system fully levitated on active magnetic bearings. Mechatronics, 24: 274-286.

Wang, J. and L. Xu, 2009a. Analysis and modeling of a switching power amplifier for magnetic bearing. Proceedings of the 4th IEEE Conference on Industrial Electronics and Applications, May 25-27, 2009, Xi'an, China, pp: 2257-2261.

Wang, J. and L. Xu, 2009b. System model of three-level switching power amplifier for magnetic bearing. Proceedings of the International Conference on Measuring Technology and Mechatronics Automation, Volume 2, April 11-12, 2009, Zhangjiajie, China, pp: 708-711.

Wang, J. and L. Xu, 2010a. Equivalent mathematical models of switching power amplifier for magnetic bearing. Trans. China Electrotech. Soc., 25: 53-64.

Wang, J. and L. Xu, 2010b. Modeling and control of system model for switching power amplifier of magnetic bearing. China Mech. Eng., 21: 477-481.

Yu, W., Y. Fan, S. Liu and D. Li, 2010. Research on MATLAB simulation of three level power amplifier for magnetic bearing. Proceedings of the Asia-Pacific Power and Energy Engineering Conference, March 28-31, 2010, Chengdu, China, pp: 1-4.

Zhang, L., J. Fang and G. Liu, 2005. Modeling and simulation of the switching power amplifier for magnetic suspending flywheel. Proceedings of the 8th International Symposium on Magnetic Suspension Technology, September 17-19, 2005, Dresden, Germany, pp: 240-244.

Zhong, Z.X. and C.S. Zhu, 2013. Vibration of flexible rotor systems with two-degree-of-freedom PID controller of active magnetic bearings. J. Vibroeng., 15: 1302-1310.

Zhou, D. and C.S. Zhu, 2010a. Failure mechanism of one kind of three-level PWM switching power amplifier for active magnetic bearings. Proceed. CSEE, 30: 103-110.

Zhou, D. and C.S. Zhu, 2010b. [Modulations of current-mode switching power amplifier for active magnetic bearings]. Ji Xie Gong Cheng Xue Bao, 46: 1-8 (In Chinese).

Zhou, D., C.S. Zhu and D. Wang, 2012. Force gain of a flux control power amplifier for active magnetic bearings. Trans. China Electrotech. Soc., 27: 188-195.